

Temperature dependent resonances in superconductor photonic crystal

C. H. Raymond Ooi and Qihuang Gong

Citation: *J. Appl. Phys.* **110**, 063513 (2011); doi: 10.1063/1.3639288

View online: <http://dx.doi.org/10.1063/1.3639288>

View Table of Contents: <http://jap.aip.org/resource/1/JAPIAU/v110/i6>

Published by the [American Institute of Physics](#).

Additional information on J. Appl. Phys.

Journal Homepage: <http://jap.aip.org/>

Journal Information: http://jap.aip.org/about/about_the_journal

Top downloads: http://jap.aip.org/features/most_downloaded

Information for Authors: <http://jap.aip.org/authors>

ADVERTISEMENT



AIP Advances

Now Indexed in
Thomson Reuters
Databases

Explore AIP's open access journal:

- Rapid publication
- Article-level metrics
- Post-publication rating and commenting

Temperature dependent resonances in superconductor photonic crystal

C. H. Raymond Ooi^{1,a)} and Qihuang Gong²

¹Department of Physics, University of Malaya, Kuala Lumpur 50603, Malaysia

²State Key Laboratory for Mesoscopic Physics and Department of Physics, Peking University, Beijing 100871, China

(Received 28 June 2011; accepted 13 August 2011; published online 22 September 2011)

We show that it is possible to obtain large field transmission through a periodic structure at frequencies where the field is lossy in a finite temperature superconductor. The feat is accomplished by using thin superconducting layers. This makes the superconductor photonic crystal useful for transmitting signals over larger distances at higher temperature. Narrow transmission resonances due to surface plasmon effect are damped more quickly with increasing temperature than broader transmission bands. The temperature dependence is useful, particularly for developing optothermal sensors in terahertz and far infrared regimes. © 2011 American Institute of Physics.

[doi:10.1063/1.3639288]

I. INTRODUCTION

Photonic crystals (PC) has been widely studied theoretically and developed for commercial applications using existing semiconductor technology. A defect in a photonic crystal serves as a microcavity that provides quantum electrodynamics (QED) effects, such as modification of the fundamental properties of radiation emitted by atoms and molecules interacting with the structurally controlled vacuum fields.¹ The QED effect has been utilized to make low threshold micro-lasers² and light emitting diodes (LED). The highly dispersive property of photonic crystal fiber has been used to generate ultra-wide bandwidth light source.

The use of superconducting materials in photonic crystals opens up new possibilities, due to the dependence of the optical properties of superconductors on temperature and magnetic field. Recent work shows the existence of a superpolariton gap in a superconductor-dielectric superlattice³ only for light with H-polarization or TM mode. It was realized that the gap falls in the infrared regime. By using certain structural parameters and high T_c superconductors, it is possible to create a low frequency gap with size of about 10^{13} Hz (10 THz) and a superpolariton gap is in the 10^{14} Hz (mid-infrared). The low frequency gap can be used to manipulate THz radiation, while the superpolariton gap is useful for controlling infrared radiation and serves as a heat screen.

In this paper, we incorporate superconducting layers into a dielectric/semiconductor crystal, as shown in Fig. 1, and study the linear optical responses of the photonic crystal. The structure has temperature dependent peaks in the dispersion, reflectance, transmittance, and surface-plasmon effect that can be used as sensors or switches in optical networks and is integrated with mid-infrared lasers for various applications. In a lot of recent works,^{4–12} temperature dependent photonic crystals were based on Casimir-Gorter relation,¹³ which provides an unrealistic description of the temperature dependence, since it is not valid for temperature above the

transition temperature T_c . We present a correct temperature dependence for the superconducting parameters that enables realistic analysis of the optical properties across the T_c .

II. OPTICAL RESPONSE AND TEMPERATURE DEPENDENCE

The optical response of the superconductor in layer 2 of the superlattice can be well described by the two-fluid model¹³ and the local London's theory. The theory is applicable to high-temperature superconductors. Hence, the linear response of the superconductor can be described by the complex conductivity

$$\sigma(\omega, T) = \sigma \left[\frac{f_n}{1 + (\omega\tau)^2} + i \left(\frac{f_n\omega\tau}{1 + (\omega\tau)^2} + \frac{f_s}{\omega\tau} \right) \right], \quad (1)$$

where $\sigma = n\tau e^2/m$ is the normal d.c. conductivity, $f_s(T) = \frac{n_s(T)}{n} = 1 - f_n$ is the proportion of superfluid (subscript "s") depends on temperature T , n is the total electron density, and n_s is the superelectron density. The dielectric function of the superconductor is obtained from $\epsilon_s(\omega, T) = 1 + \frac{i\sigma(\omega, T)}{\epsilon_0\omega}$. The imaginary part $\frac{(1-f_s)z}{1+z^2} + \frac{f_s}{z}$ contributes to the dispersion, where $z = \omega\tau$. The real part gives absorption and can be minimized at low temperature and high frequency.

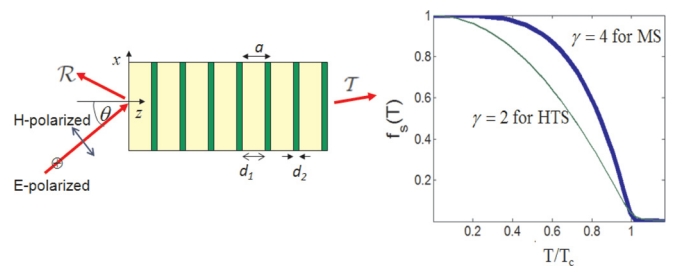


FIG. 1. (Color online) Finite bi-layer superconductor photonic crystal showing arbitrary angle of incidence θ and the continuous temperature-dependent superfluid fraction f_s for high temperature superconductor (HTS) and metallic superconductor (MS).

^{a)}Author to whom correspondence should be addressed. Electronic mail: bokooi73@yahoo.com.

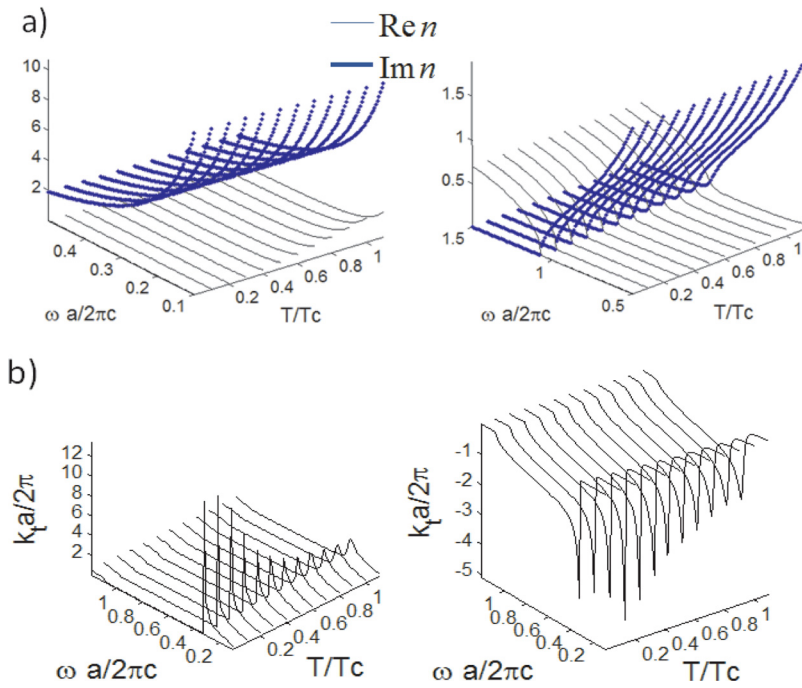


FIG. 2. (Color online) Temperature variations of the (a) refractive index of superconductor and (b) tangential wavevector $k_t = \frac{\omega}{c} \sqrt{\frac{\epsilon_1 \epsilon_2}{\epsilon_1 + \epsilon_2}}$ ($\epsilon_2 = \epsilon_s(\omega, T)$, $\epsilon_1 = 10$) at the interface of the superconductor-dielectric with plasmonic resonance. We use temperature-related parameters $\gamma = 2$ and $S_2 = 170$, with $a = 800 \text{ nm}$, $\tau_2 = 1/(8 \times 10^{13})$, $n = 10^{27}$, and $n_2 = 2n$.

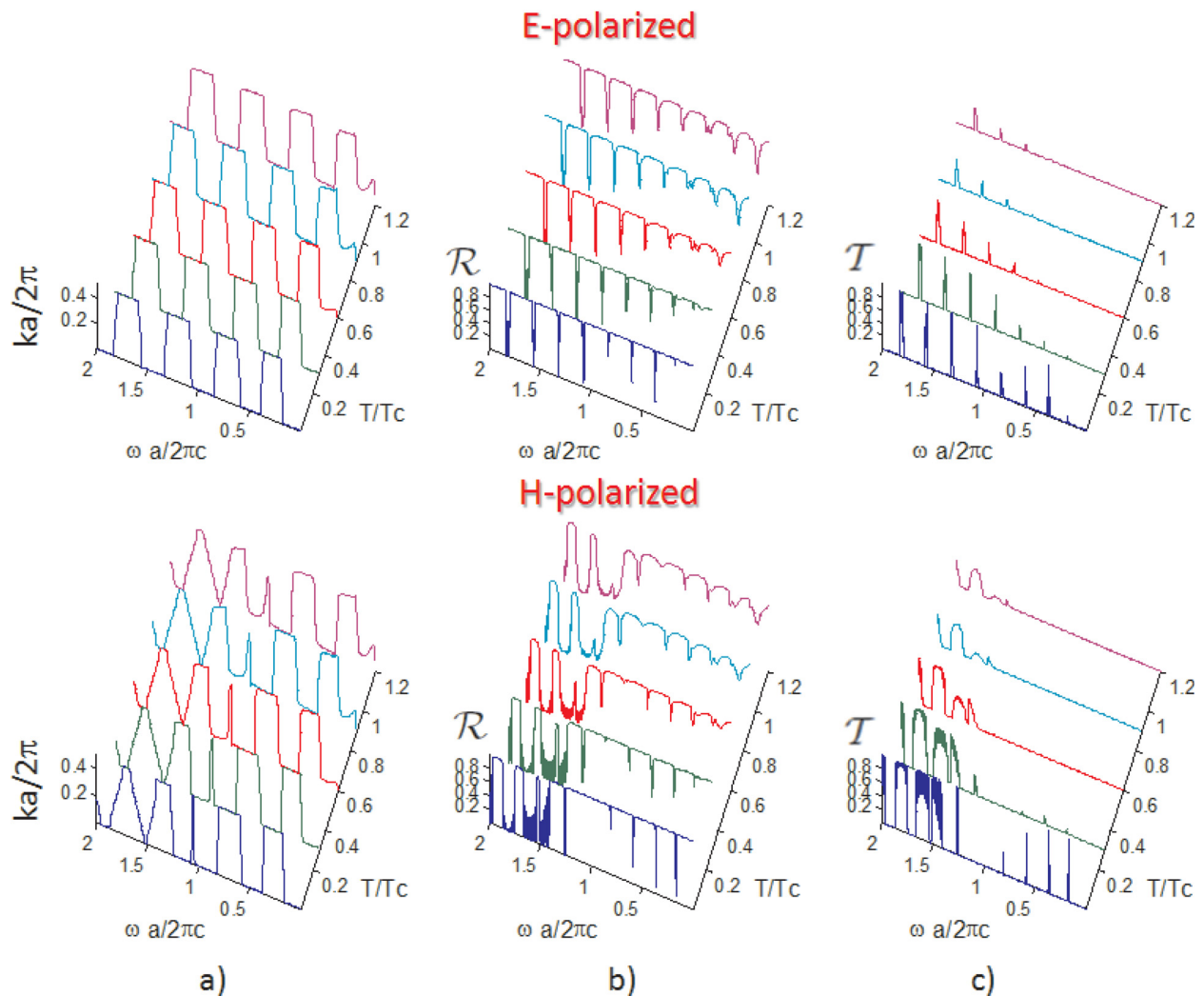


FIG. 3. (Color online) (a) photonic band structure dispersion, (b) reflectance \mathcal{R} , (c) transmittance \mathcal{T} at different temperatures across T_c . Layer 1 is a dielectric with $\epsilon_1 = 10$. Layer 2 is a superconductor. The parameters used are (subscript 2 indicates layer 2): angle of incidence $\theta = \pi/4$, $\tau_2 = (8 \times 10^{13})^{-1} \text{ s}$, $n = 10^{27}$, and $n_2 = 2n$, with temperature-related parameters $\gamma = 2$ and $S_2 = 170$ and structural parameters $N = 15$, $a = 800 \text{ nm}$, and $d_1 = 500 \text{ nm}$.

Periodic tunnelling effect, $d_2=100$ nm

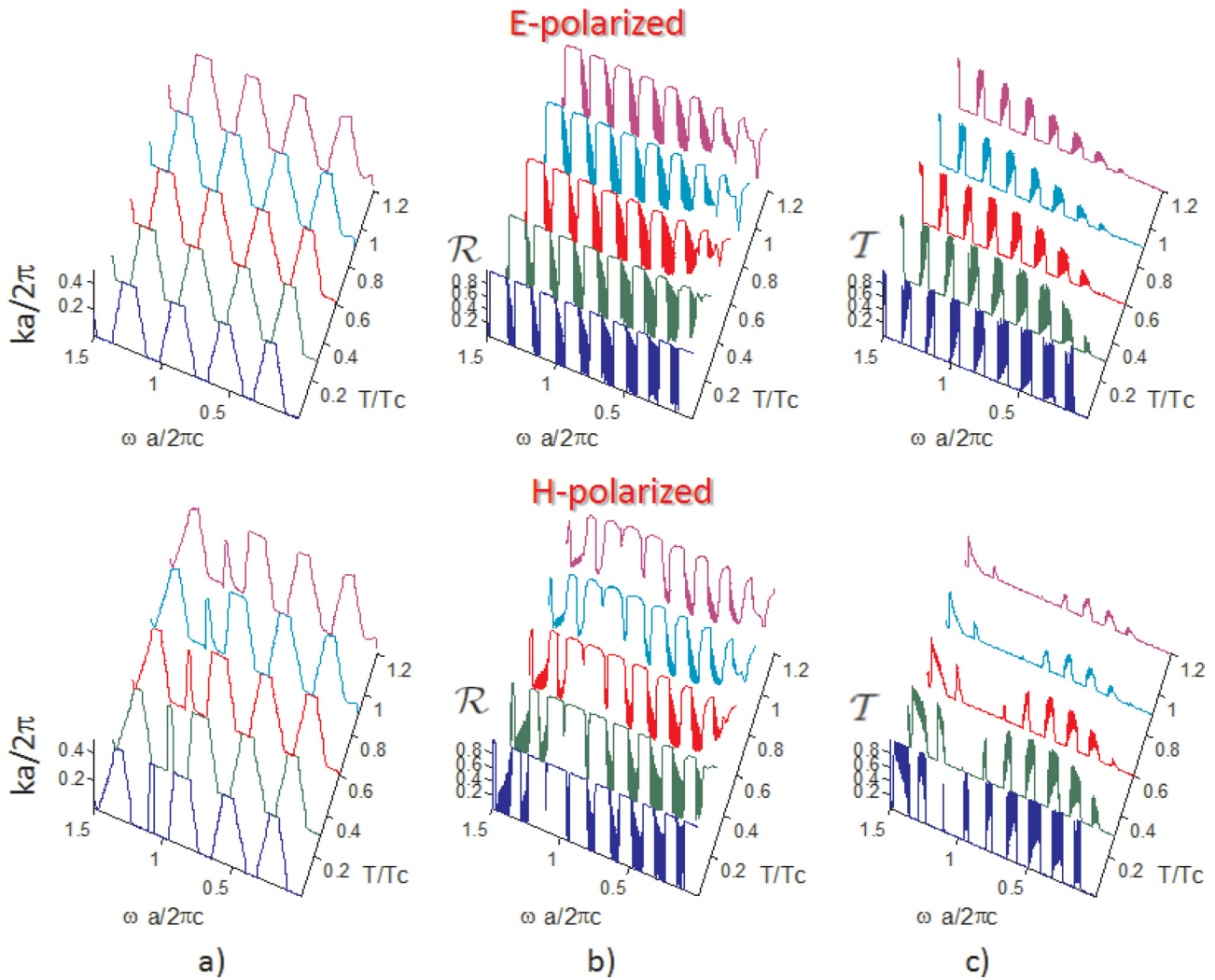


FIG. 4. (Color online) Same as Fig. 3 except with narrower superconductor layers $d_2 = 100$ nm. (a) Photonic band structure dispersion, (b) reflectance \mathcal{R} , and (c) transmittance \mathcal{T} at different temperatures across T_c . Layer 1 is a dielectric with $\epsilon_1 = 10$. Layer 2 is a superconductor.

At high frequency, $(\omega\tau)^2 \gg 1$ and $\sigma(\omega, T) \simeq \sigma \left[\frac{f_n}{(\omega\tau)^2} + i\frac{1}{\omega\tau} \right]$, with the ratio of imaginary to real part becoming $\frac{\omega\tau}{f_n}$, which is large and the superconductor is more transparent especially at low T . On the other hand, at low frequency, $(\omega\tau)^2 \ll 1$ we have $\sigma(\omega, T) \simeq \sigma \left[\frac{f_n}{T} + i\left(\frac{f_n}{\omega\tau}\right) \right]$, with the ratio of the imaginary to the real part becoming $\frac{f_n}{f_n\omega\tau}$, which is large and more transparent, especially at low T .

The London penetration depth at $T = 0$ is $\lambda_L = \sqrt{\frac{m}{\mu_0 e^2 n}}$. The well-known temperature dependence in $n_s(T)$ is given by the Gorter-Casimir relation $n_s(T)/n = 1 - x^4$. This relation becomes negative, which is unphysical for $x = \frac{T}{T_c} > 1$. To study the temperature dependence near the transition temperature, we modify the Gorter-Casimir relation by removing the cusp based on a simple expression in the Appendix of Ref. 14.

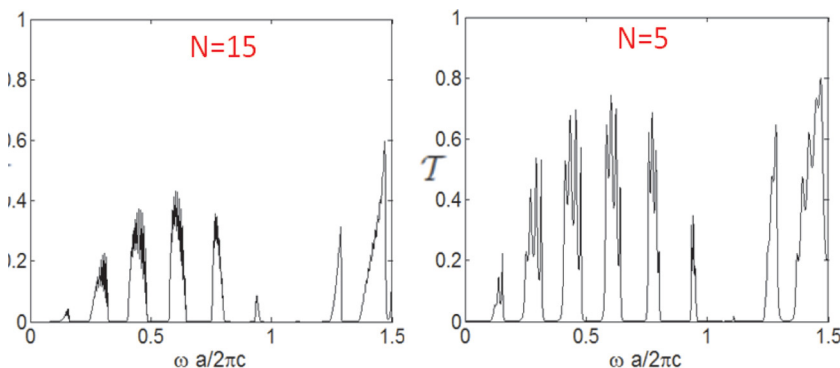


FIG. 5. (Color online) Transmission for different N number of layers at $T = 0.8T_c$ for the H-polarized case. Other parameters are the same as Fig. 4.

dielectric with phonon-polariton dispersion

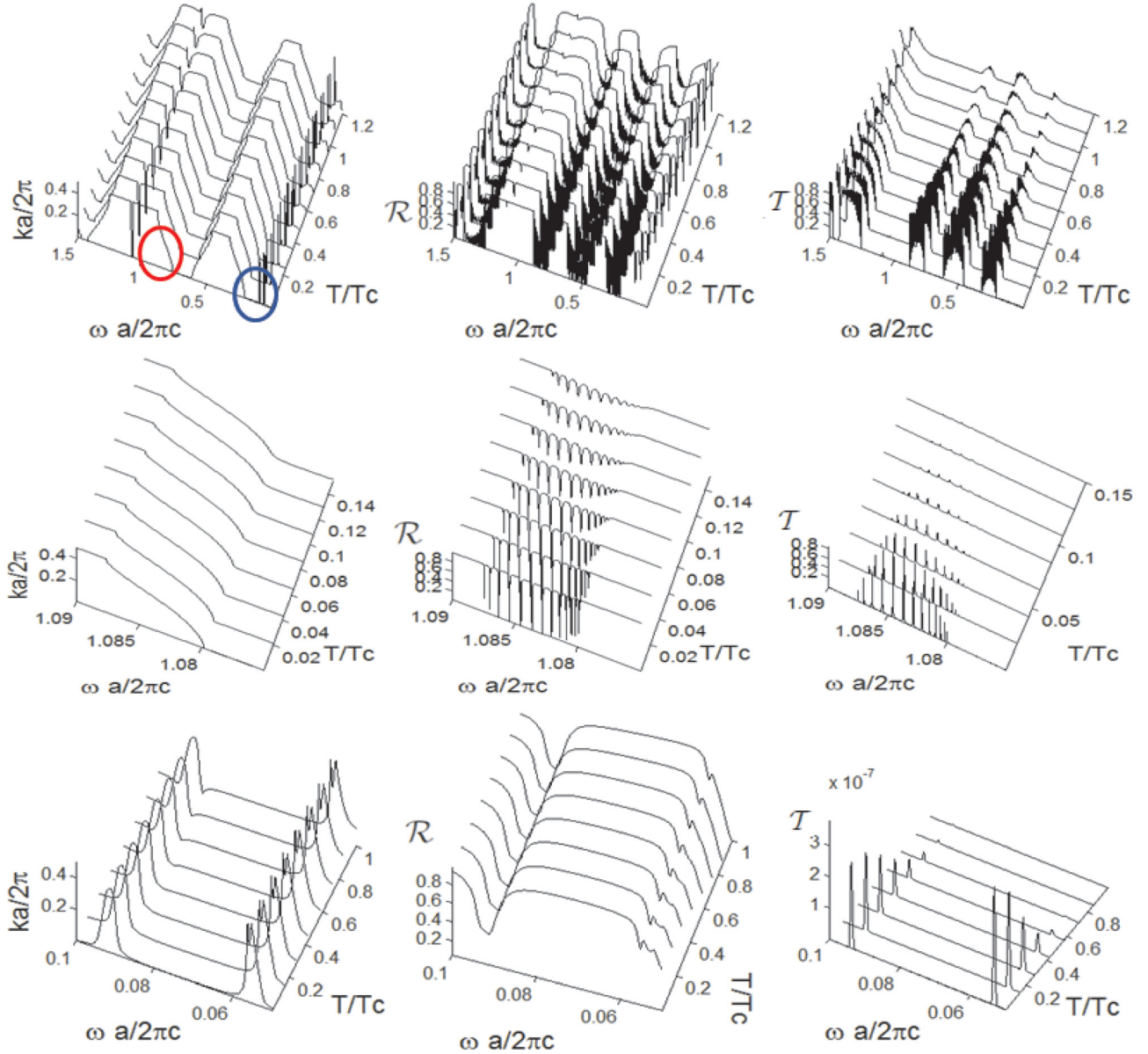


FIG. 6. (Color online) Temperature dependence of narrow transmission peaks for the H-polarized case. Same as Fig. 4, except layer 1 with constant dielectric has been replaced by frequency dependent dielectric function describing phonon-polariton dispersion with parameters $\omega_T = 87$ meV, $\epsilon_0 = 7.65$, $\epsilon_\infty = 2.99$, and $\gamma = 2\pi 3.6512 \times 10^{11} \text{ s}^{-1}$. The second and third rows magnify the lower circle region of low frequency (around 0.08) bandgap and the upper circle region (around 1.00) of polariton dispersion, respectively.

$$f_s(T) = \frac{1}{2} \left[1 - x^4 + \sqrt{(1 - x^4)^2 + \frac{x^3}{S}} \right], \quad (2)$$

where S is a positive number chosen to smoothen the cusp. This function is always positive and provides a simple qualitative description of the temperature dependence.

The first layer is a dielectric material to be specified later. The dispersion of the photonic crystal can now be obtained by using the Bloch-Floquet theorem:¹⁵

$$\begin{aligned} \cos Ka &= \cos(k_{1z}d_1) \cos(k_{2z}d_2) \\ &- \frac{1}{2} \left(r_p + \frac{1}{r_p} \right) \sin(k_{1z}d_1) \sin(k_{2z}d_2). \end{aligned} \quad (3)$$

Here, r_p is $r_E = \frac{k_{2z}}{k_{1z}}$ for incident light with E-polarization and $r_H = \frac{k_{2z}}{k_{1z}} \frac{k_1^2}{k_2^2}$ for H-polarization, where $k_{jz} = (\omega/c) \sqrt{\epsilon_j \mu_j - \epsilon \mu \sin^2 \theta}$ are the z-component wavevectors in the superconductor ($j=2$) and dielectric ($j=1$) layers. The solution for K from Eq. (3) enables the reflection and transmission coefficients, $r(\omega)$ and $t(\omega)$ to be computed by using Abeles theory.¹⁶ The transmission $\mathcal{T}(\omega) = |t(\omega)|^2$ and reflection $\mathcal{R}(\omega) = |r(\omega)|^2$ spectra can then be obtained. Further details can be found in Ref. 3. For very thin superconductor (nanolayers), the dispersion relation may be simplified to $\cos Ka = \cos(k_{1z}d_1) - \frac{1}{2} \left(r_p + \frac{1}{r_p} \right) k_{2z}d_2 \sin(k_{1z}d_1)$.

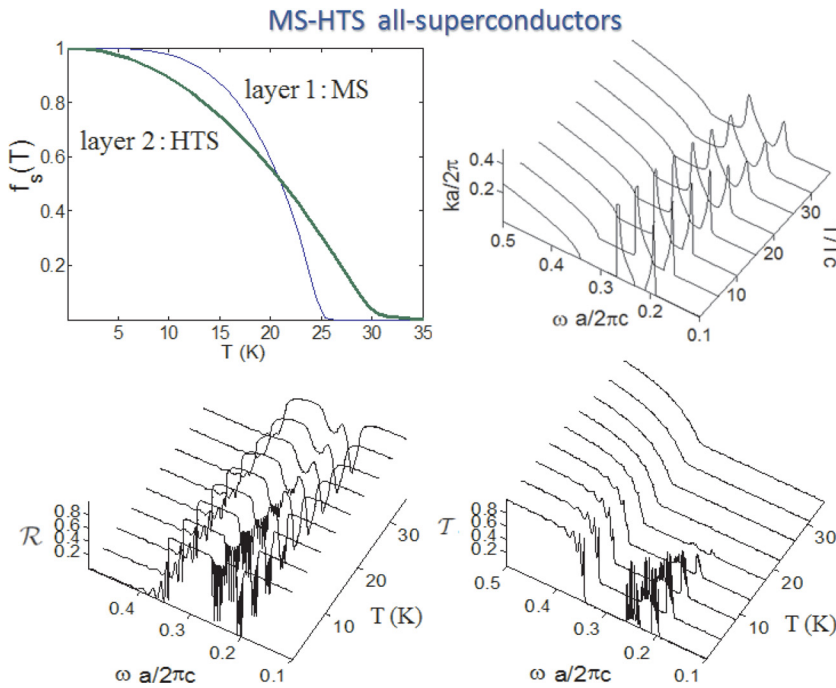


FIG. 7. (Color online) Superfluid fraction, photonic band structure, reflection, and transmission for the all-superconductor structure with MS as layer 1 and HTS as layer 2. Layer 1 has parameters of $\tau_1 = (7 \times 10^{13})^{-1} s$ and $n_1 = 10^{27}$, with temperature dependence parameters $S_1 = 500$ and $\gamma = 4$, and structural parameters $N = 15$, $a = 200 \text{ nm}$, and $d_1 = 100 \text{ nm}$. The parameters for layer 2 are the same as in Fig. 3. The transition temperatures are $T_{c1} = 25 \text{ K}$ and $T_{c2} = 30 \text{ K}$.

III. RESULTS AND DISCUSSIONS

The real and imaginary parts of the refractive index $n_s(\omega) = \sqrt{\epsilon_s(\omega)}$, plotted in Fig. 2(a), show that the superconductor is highly absorptive for $\omega a/2\pi c = a/\lambda < 1$. The curves do not vary significantly with temperature except some rounding off near the T_c . An interesting result is found in the superplasmonic enhancement by the superconductor-dielectric interface. The tangential wavevector of the surface plasmon $k_t a/2\pi = a/\lambda_{\text{eff}} = 15$ in Fig. 2(b) shows a resonance at $a/\lambda = 0.3$ close to absolute zero. This is equivalent to $\lambda/\lambda_{\text{eff}} = 50$, a significant subwavelength enhancement. Unfortunately, the imaginary part is also very large and the enhancement factor drops with increasing temperature.

The results for transmission \mathcal{T} and reflectance \mathcal{R} are shown in Fig. 3 for E- and H-polarizations. For certain parameters, $\theta = 45^\circ$ and $d_2 = 300 \text{ nm}$ with E-polarized light, we find quasiperiodic transmission peaks almost equally spaced. This feature could be useful for obtaining a frequency comb from a supercontinuum light source. However, the height of those peaks at low frequencies gradually decrease as the temperature increases toward T_c . Such periodic peaks almost do not appear for finite temperatures in H-polarization. The dispersion also shows a single defect mode with very narrow transmission. However, it is found only at temperature close to absolute zero and drops very rapidly as the temperature increases towards T_c .

When the superconducting layer is made narrower, $d_2 = 100 \text{ nm}$, the transmission peaks increase, especially at lower frequencies (see Fig. 4). This might seem surprising and counterintuitive at first, since the imaginary part of $n_s(\omega)$ is much greater than the real part for $a/\lambda < 1$, according to Fig. 2(a). It is due to the periodic tunneling of the evanescent/damped fields from the narrow superconducting

layers into the dielectric layers that enable the continuity in the field propagation through the dielectric layer. A narrow transmission peak appears at $a/\lambda = 1.1$ for the H-polarized case, due to the tangential component of the E-field, possibly connected to the surface plasmon resonance. We also find that the narrower superconducting layer (Fig. 4) and the small number of bilayers N (Fig. 5) give large transmission peaks that are useful for temperature sensing.

The large transmission effect also persists for semiconductor dielectric material around phonon-polariton resonance. Figure 6 shows the effects of phonon-polariton resonance in layer 1 using $\epsilon_d(\omega) = \epsilon_\infty + \frac{\omega_p^2}{(\omega_T^2 - \omega^2 - i\gamma\omega)}$, where $\omega = \sqrt{\omega_L^2 - \omega_T^2}$ is the photon-phonon coupling strength and ω_L and ω_T are frequencies of the transverse and longitudinal optical phonons. The results provide a closer look at how the narrow defect peaks for the H-polarized case change with temperature. The two narrow peaks within the low frequency gap with very low transmission could be useful for producing few photon sources at very specific frequencies for use in quantum information technology. At a higher frequency, the narrow dispersion band has regularly spaced ultranarrow peaks with height that reduces very rapidly within a small temperature range, although the photonic band structure appears to be essentially unchanged. By setting a transmission level to a triggering device, the structure can be used as a sensitive low-temperature switch/sensor.

Figure 7 shows the band structure and the spectrum for the all-superconductors structure with different transition temperatures. Layer 1 and 2 are thin metallic superconductor (MS) and thin high- T_c superconductor (HTS), respectively. The transmission peaks are damped as the temperature increases, despite the nanometer thickness. This shows that a dielectric layer, even though around polariton resonance, is necessary to sustain long distance transmission.

IV. POTENTIAL APPLICATIONS

The effects found by introducing superconducting strips into semiconductors are useful for several applications. Since $a = 800 \text{ nm}$ and the interesting features lie within $a/\lambda < 1$, the useful operating frequency is in the range of infrared and terahertz. In photonic circuits, the narrow transmission peaks of the superlattice can filter out narrowband of light. The narrow wavelength filter would also be useful for developing a narrow wavelength source for spectroscopic studies, sensing, and imaging. The wavelengths selected by the narrowband in the photonic crystal can be manipulated and undergo non-linear frequency conversion to and from the C-band for free space communication technologies.¹⁷

The small group velocity serves as an optical buffer to control the delay of transmitted and reflected signal.¹⁸ The slow light modes have wavelengths compatible with the wavelengths of efficient quantum cascade lasers¹⁹ in the mid-infrared and, therefore, can be integrated as slow light modulator (SLM) into monolithic devices for developing photonic chips, gas sensors, and for high precision spectroscopy. The temperature dependence of the superconductor makes it possible to use the slow light effect for measuring temperature. Conversely, we may also have temperature tunable delay and optothermal switch.

V. CONCLUSIONS

We have analyzed the temperature dependence of the finite superconductor-dielectric photonic band structure. Analysis of the band structure, the transmission, and reflection spectra shows interesting features, such as temperature-sensitive narrow transmission peaks. These features provide insights for designing optothermal sensors or switches and temperature controlled photon sources that operate at finite temperatures. We study how these optical responses depend on the relative thickness of the layers and the intrinsic parameters of the superconducting and dielectric materials. The transmission peaks can be increased by using a narrower superconducting layer and reducing the number of bilayers.

Thus, the temperature dependence of a superconducting photonic crystal opens up exciting possibilities for new photonic devices.

ACKNOWLEDGMENTS

This work is supported by Ministry of Higher Education (MOHE)/University Malaya HIR grant A-000004-50001 and the MOHE FRGS grant FP005/2010B.

- ¹S. John and T. Quang, *Phys. Rev. A* **50**, 1764 (1994).
- ²H. Altug, D. Englund, and J. Vukovic, *Nat. Phys.* **2**, 484 (2006).
- ³C. H. Raymond Ooi, T. C. Au Yeung, C. H. Kam, and T. K. Lim, *Phys. Rev. B* **61**, 5920 (2000).
- ⁴L. Feng, X.-P. Liu, J. Ren, Y.-F. Tang, Y.-B. Chen, Y.-F. Chen, and Y.-Y. Zhu, *J. Appl. Phys.* **97**, 073104 (2005).
- ⁵H. Takeda and K. I. Yoshino, *Phys. Rev. B* **67**, 245109 (2003); T.-H. Pei and Y.-T. Huang, *Jpn. J. Appl. Phys.* **46**, L593 (2007).
- ⁶P. Li, Y. Liu, Y. Meng, and M. Zhu, *J. Opt. A, Pure Appl. Opt.* **11**, 114014 (2009).
- ⁷C. Cheng, C. Xu, T. Zhou, X.-F. Zhang, and Y. Xu, *J. Phys.: Condens. Matter* **20**, 275203 (2008).
- ⁸T.-H. Pei and Y.-T. Huang, *J. Appl. Phys.* **101**, 084502 (2007).
- ⁹C. J. Wu, C. L. Liu, W. K. Kuo, *J. Electromagn. Waves Appl.* **23**, 1113 (2009); H.-T. Hsu, F.-Y. Kuo, and C.-J. Wu, *J. Appl. Phys.* **107**, 053912 (2010).
- ¹⁰K. B. Thapa, S. Srivastava, and S. Tiwari, *J. Supercond. Novel Magn.* **23**, 517525 (2010).
- ¹¹A. N. Poddubny, E. L. Ivchenko, and Yu. E. Lozovik, *Solid State Commun.* **146**, 143 (2008); Yu. E. Lozovik, S. L. Eiderman, and M. Willander, *Laser Phys.* **17**, 1183 (2007).
- ¹²N. N. Dadoenkova, A. E. Zabolotin, I. L. Lyubchanskii, Y. P. Lee, and Th. Rasing, *J. Appl. Phys.* **108**, 093117 (2010).
- ¹³T. van Duzer and C. W. Turner, *Principles of Superconductive Devices and Circuits* (Prentice Hall, London, 1981).
- ¹⁴A. N. Jordan, C. H. Raymond Ooi, and A. Svidzinsky, *Phys. Rev. A* **74**, 032506 (2006).
- ¹⁵C. Kittel, *Introduction to Solid State Physics*, 6th ed. (Wiley, New York, 1986).
- ¹⁶M. Born and E. Wolf, *Principles of Optics*, 7th ed. (Pergamon, New York, 1999).
- ¹⁷K. F. Büchter, H. Herrmann, C. Langrock, M. M. Fejer, and W. Sohler, *Opt. Lett.* **34**, 470 (2009).
- ¹⁸C. H. Raymond Ooi and C. H. Kam, *J. Opt. Soc. Am. B* **27**, 458 (2010).
- ¹⁹R. Colombelli, K. Srinivasan, M. Troccoli, O. Painter, C. F. Gmachl, D. M. Tennant, A. M. Sergent, D. L. Sivco, A. Y. Cho, and F. Capasso, *Science* **302**, 1374 (2003).